6-13-2007

Quantum Size Effect and Biased Diffusion of Gravitationally Bound Neutrons in a Rough Waveguide

R. Adhikari
University of Rhode Island

Y. Cheng
University of Rhode Island

A. E. Meyerovich
University of Rhode Island, sfo101@uri.edu

V. V. Nesvizhevsky

Citation/Publisher Attribution

Adhikari, R., Cheng, Y., Meyerovich, A. E., & Nesvizhevsky, V. V. (2007). Quantum Size Effect and Biased Diffusion of Gravitationally Bound Neutrons in a Rough Waveguide. *Phys. Rev. A*, *75*(6), 063613, 1-12. doi: 10.1103/PhysRevA.75.063613
Available at: http://dx.doi.org/10.1103/PhysRevA.75.063613

Quantum Size Effect and Biased Diffusion of Gravitationally Bound Neutrons in a Rough Waveguide

Quantum size effect and biased diffusion of gravitationally bound neutrons in a rough waveguide

R. Adhikari, Y. Cheng, and A. E. Meyerovich
Department of Physics, University of Rhode Island, Kingston, Rhode Island 02881-0817, USA

V. V. Nesvizhevsky
ILL, Grenoble, France

(Received 26 April 2007; published 13 June 2007)

A comprehensive theory of gravitational quantum states of ultracold neutrons in a rough waveguide is presented. The theory covers recent experiments in which the ultracold neutrons were beamed between a mirror and a rough scatterer and absorber. The results are in very good agreement with experimental data. The analysis is based on a recently developed theory of quantum transport in waveguides with rough absorbing and scattering walls. The calculation is done using two methods: an exact transport equation and a simplified model of biased scattering-driven diffusion of neutrons between quantum states. Both sets of results are in excellent agreement with each other. The exit neutron count is sensitive to the amplitude and the correlation radius (lateral size) of surface inhomogeneities and to the overall time of flight (length of the waveguide). The results indicate that it is possible to choose the waveguide parameters in such a way so to observe the quantum size effect in neutron count—the quantum steps that correspond to individual quantum states—even in a weak roughness regime. Away from the obvious limiting cases, the results are not very sensitive to the ratio of the particle energy to the absorption threshold. The main unresolved issue, which is related to a complexity of required calculations for a "real" experimental cell, is the lack of accurate information on the occupation numbers of neutrons entering the waveguide. Our analysis indicates that the initial occupancies of all gravitational states are expected to be the same except for the smallest values of the waveguide width.

DOI: 10.1103/PhysRevA.75.063613 PACS number(s): 03.75.Be, 03.65.Ta, 81.07.St

I. INTRODUCTION

One of the recent discoveries in neutron physics was the experimental observation of the quantization of motion of ultracold neutrons in a gravitational field [1]. By itself, the quantization of particle motion in a linear potential is well known and has already been observed for other particles (for example, for spin-polarized atomic hydrogen in a magnetic field with a linear gradient [2]). However, Earth's gravitational field is so weak and the energies of the corresponding discrete quantum states for neutrons are so low (on the scale of 1 peV) that the observation of such states is indeed a major experimental breakthrough. Besides, these low-energy, gravitationally quantized neutrons could become an invaluable tool for measuring the fundamental forces in the μm range [3–5].

Experimental resolution of gravitational states was achieved by collimating a horizontal beam of gravitationally quantized particles by two mirrors: a rough one on the top and an ideal one on the bottom. The neutron reflection was locally specular as long as the vertical component of the velocity did not exceed a certain threshold value; the neutrons with vertical velocities above this threshold were absorbed. The neutrons entering the slit had a large horizontal component of velocity and a much smaller vertical component. The scattering of neutrons by the rough upper mirror caused a rotation of this initially horizontal velocity. The rotation of the velocity led, in turn, to an increase in its vertical component and, eventually, to absorption of the scattered neutrons. Only the neutrons in the lowest gravitational states, which could not reach the upper (rough) mirror, were not absorbed and were counted by an exit neutron counter.

This neutron problem is different in two aspects from typical quantum transport problems with scattering by random surfaces (see, e.g., the short review in Ref. [6] and references therein). First, here the wall collision leads not only to particle scattering and randomization of momenta, but also to particle absorption. Second, the cell is relatively short and we should solve a transport problem with initial conditions rather than evaluating a stationary particle flux at $t \to \infty$ as in standard transport problems. This second peculiarity makes this problem somewhat similar to the problem of particle propagation through a finite layer of a random medium with above-barrier scattering [7]. The latter problems were studied mostly for one-dimensional (1D) systems; we do not know any publications dealing explicitly with quantized quasi-2D systems with a large number of discrete quantum states. This makes the results below not only useful for neutron experiments, but also interesting from a theoretical standpoint.

Recently we analyzed the propagation of quantized neutrons in a rough waveguide [8] with the aim of describing the experiment [1]. We calculated the absorption rates for direct roughness-driven transitions from quantized gravitational states into a continuum (direct absorption). The results were not very encouraging: the weak roughness of the waveguide surface was not sufficient for resolving even a couple of gravitational states. Resolving these states would require either an increase in the length of experimental cell by more than an order of magnitude or making the surfaces with strong roughness. The former option is inconceivable experimentally, and the latter one would result in a large shift and broadening of quantized levels which, in turn, could make the results useless for precise calibration in future applications.

Although the main equations of Ref. [8] are quite general, the computational results have restricted parametric applica-

bility and do not, by any means, preclude the possibility of experimental resolution of individual gravitational states even within the existing experimental technique. The calculations took into account only the direct scattering-driven transitions from discrete quantum states into a continuum above the absorption threshold. We knowingly disregarded all indirect absorption processes via gradual upward diffusion of particles among the discrete states. The disregard of indirect processes always underestimates the absorption rate. The balance between direct and indirect absorption processes is determined by the scale (correlation radius R) of roughness. The coarser the roughness, the stronger is the suppression of direct absorption processes. As a result, the applicability of the theory [8] is restricted only to a low-scale roughness ($R \lesssim 0.05$ μm) for which direct transitions are dominant.

In addition, according to experiments [1], the absorption rate was not very sensitive to the absorption threshold. This could indicate that in these experiments the absorption via the intermediate states was more effective than the direct transitions from the lower states into continuous spectrum. Indeed, when indirect processes are dominant and the lifetime of the higher states drops rapidly with an increase in the quantum number, the exact value of the absorption threshold loses importance: the threshold-independent transition from a lower state into an intermediate one requires much more time than the final stages of absorption which depend on the threshold position.

At first glance, the use of coarser surfaces with larger inhomogeneities should make the interstate transitions and, therefore, the depletion of neutrons more difficult. This is not necessarily true: the increase of the correlation radius (lateral size) of the surface inhomogeneities R allows one to increase simultaneously the amplitude (height) of roughness ℓ while still remaining in the weak roughness domain $\ell \ll R, l_0$ until R becomes comparable to l_0; a further increase in R cannot be accompanied by an increase in ℓ. (In this particular case, l_0 is the size of the lowest gravitationally bound state; see below.) We believe that this could allow an observation of the quantum size effect for neutrons in the gravitational field—the stepwise dependence of the neutron count on the spacing between the walls—using the weak roughness which does not distort the energy levels themselves. The results below include both direct and indirect absorption processes and cover the whole range of values of R from the low-scale roughness of [8] to coarse surfaces $R \gtrsim l_0$ and provide a good description of experimental data.

The paper has the following structure. In the next section, we introduce the main equations and relevant notations. In Sec. III we develop a biased diffusion model for calculation of neutron depletion via the intermediate states. The results for this model are discussed in Sec. IV. Though the semianalytical results of the biased diffusion model are very transparent and the computation times are very fast, these results should be supplemented by solving the full transport equation, especially for the most important combinations of parameters. This is done in Sec. V in which we also discuss the accuracy of the biased diffusion model. Section VI deals with a comparison with experimental data including a detailed discussion of various factors which affect the accuracy. In Sec. VII we summarize the conclusions.

II. MAIN EQUATIONS AND NOTATIONS

In this section we introduce the notations and dimensionless variables, which are common to the field, and give the main equations. In a typical experiment, a beam of ultracold neutrons with energy E propagates between rough and ideal mirrors with absorption threshold U_c. The main experimental result is the number of neutrons exiting the collimator as a function of the spacing between the walls H, particle energy E, absorption threshold U_c, and the mirror roughness.

The distances z and the energies of the quantum levels ϵ_n are often measured in units of l_0 and e_0, $s=z/l_0$, and $\lambda_n = \epsilon_n/e_0$, where $l_0=\hbar^{2/3}(2m^2g)^{-1/3} \sim 5.871$ μm and $e_0=mgl_0 \sim 0.602$ peV $\sim 9.6366 \times 10^{-32}$ J are the size and the gravitational energy of a neutron in the lowest quantum state in the *infinite* gravitational trap. In these units, the typical overall kinetic energy of particles in the beam E and the absorption threshold U_c are very large, $1.4 \times 10^5 < e = E/e_0 < 8.7 \times 10^5$ and $u_c = U_c/e_0 \sim 1.4 \times 10^5$. In experiment, the ratio $\chi = u_c/e$ changed between

$$0.16 \lesssim \chi \equiv u_c/e < 1. \tag{1}$$

This parameter shows how easy is it for a neutron to get absorbed by a wall when the direction of velocity is rotated as a result of scattering by the rough scatterer and absorber. The dimensionless distance between the walls is $h=H/l_0$.

It is also convenient to introduce the dimensionless velocities (momenta) in the beam direction along the wall (x direction) β_j, $v_j=\beta_j v_0$, $v_0=\sqrt{2gl_0}=\hbar/ml_0 \sim 1.073 \times 10^{-2}$ m/s, and $\beta_j=\sqrt{e-\lambda_j} \equiv p_j l_0$ [for lower levels, $\lambda_j \ll e$ and $\beta_j \simeq \sqrt{e}(1-\frac{1}{2}\lambda_j/e)$]. The range of kinetic energies in experiment is $370 < \sqrt{e} < 930$.

For the time units, one can choose

$$\frac{1}{\tau_0} = \frac{\sqrt{2\pi}}{4m}\frac{\hbar}{l_0^2} \approx 1148.7 \text{ s}^{-1}, \tag{2}$$

which provides the scale for the oscillation frequency of neutrons in the gravitational well. In experiment [1], the typical time of flight of neutrons through the cell is $t=L_x/V_0 \sim 2 \times 10^{-2}\kappa$ s (parameter κ is close, but not always equal to, 1 because of variations in the beam energy u_c/χ and in the cell length). Then

$$t/\tau_0 \simeq 23\kappa. \tag{3}$$

For the correlation function of surface roughness we choose the most commonly used Gaussian form

$$\zeta(x) = \ell^2 \exp(-x^2/2R^2),$$

$$\zeta(p_j - p_{j'}) = \sqrt{2\pi}\ell^2 R \exp[-(\beta_j - \beta_{j'})^2 r^2/2], \tag{4}$$

with the correlation radius $r=R/l_0$ and the amplitude $\eta = \ell/l_0$. The generalization to non-Gaussian roughness is straightforward [9]. The roughness is weak when both its amplitude and its aperture are small,

$$\eta \ll r,h. \tag{5}$$

It is convenient to characterize the aperture of roughness by the ratio of the amplitude to the correlation radius (lateral size) of inhomogeneities:

$$\gamma = \ell/R \equiv \eta/r. \tag{6}$$

Equation (4) in these units assumes the form

$$\zeta(p_j - p_{j'}) = \sqrt{2\pi} l_0^3 \gamma^2 r^3 \exp[-(\beta_j - \beta_{j'})^2 r^2/2]. \tag{7}$$

The parameters γ and κ will almost always enter the results in the combination $\gamma^2\kappa$ and, therefore, can be treated as a single parameter:

$$\sigma = \gamma^2 \kappa. \tag{8}$$

The numerical results below are presented for $\sigma=1$ unless it is explicitly stated otherwise.

III. ABSORPTION PROCESS AND BIASED DIFFUSION

Our previous results [8], which disregard the roughness-driven interstate diffusion and take into account only the direct transitions into continuous spectrum (direct absorption), are accurate for the low-scale roughness. Elsewhere, these results provide a lower bound for the absorption rate. In this section we will give analytical expressions for an upper bound for the absorption rate. This simple calculation is based on the fact that the transition rates between the states j and j', $1/\tau_{jj'} = (1/\tau_0) w_{jj'}$, rapidly increase with *both* quantum numbers j and j'. Since the rates of direct absorption processes $1/\tau_j^{(0)} = (1/\tau_0) w_j^{(0)}$ also rapidly increase with an increase in j, the lifetimes of the higher states are by orders of magnitude shorter than for the lower states. Therefore, the diffusion of particle between the energy levels has a strong upward bias and one can often disregard the downward transitions. Then the biggest hurdle for absorption of a particle from the level j is just the first jump—getting to one of the higher levels $j' > j$—with the absorption time for the state j' being very short on the scale of the $j \to j'$ jump. When this is true, a good estimate of the depletion rate of the state j is

$$\frac{1}{\tau_j} = \frac{1}{\tau_j^{(0)}} + \sum_{j'>j} \frac{1}{\tau_{jj'}} = \frac{1}{\tau_0}\left(w_j^{(0)} + \sum_{j'>j} w_{jj'} \right). \tag{9}$$

To illustrate this point, let us look at the transition probabilities between the states, $W_{jj'}$ [8]:

$$\frac{1}{\tau_{jj'}} = v_j^{-1} \zeta(p - p') U_c^2 \psi_j^2(H) \psi_{j'}^2(H), \tag{10}$$

where $\zeta(p-p')$ is the correlation function of surface roughness, U_c is the absorption threshold, and $\psi_j(H)$ are the values of the wave functions on the rough wall. To better appreciate the dependence on the scattering probabilities on the state indices j and the correlation radius of surface roughness R, which is responsible for the upward bias, let us rewrite Eq. (10) in the simplest case of an almost infinite square potential well and Gaussian inhomogeneities:

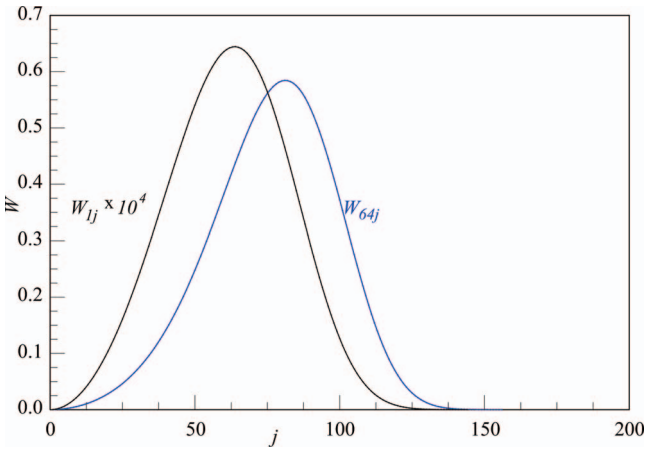

FIG. 1. (Color online) The rates of transition from the first level, w_{1j}, and from the 64th level, w_{64j}, Eq. (11), onto all other levels j for $r=1.16$, $\eta=0.116$, $\chi=0.16$, and $h=5$. Plotted are $10^4 \times w_{1j}$ and w_{64j}.

$$\frac{1}{\tau_{jj'}} = \frac{1}{\tau_0} w_{jj}, \quad w_{jj'} = \frac{\pi^4}{4} \frac{\eta^2 r}{\beta_j} \frac{j^2 j'^2}{h^6} \exp\left[-(\beta_j - \beta_{j'})^2 \frac{r^2}{2} \right], \tag{11}$$

where $h = H/l_0$ is the dimensionless spacing between the walls. This equation clearly illustrates that the probability of transitions to the higher states increases quadratically with the quantum numbers of the initial and final states j and j' and that the dominance of direct transitions into very high energy states $j' \gg j$ is restricted only by the correlation exponent which limits the momentum transfer in a transition to $\delta\beta = \beta_j - \beta_{j'} = |\sqrt{e-\lambda_j} - \sqrt{e-\lambda_{j'}}| \lesssim 1/r$. Therefore, in the cases of small correlation radii $1/r \gtrsim \sqrt{e} - \sqrt{e-u_c}$ direct transitions over the absorption threshold dominate the neutron depletion and we should return to the results of [8].

When, however, the correlation radius r is not small, the direct absorption term with $1/\tau_j^{(0)}$ in Eq. (9) becomes small in comparison with the term with the sum of interlevel transitions, which, in turn, is cut off by the condition

$$(\beta_j - \beta_{j'})^2 r^2/2 = (\sqrt{e-\lambda_j} - \sqrt{e-\lambda_{j'}})^2 r^2/2 \lesssim 1. \tag{12}$$

For not very high energy levels $\lambda_j \ll e \sim 10^5$, this condition is equivalent to

$$|\lambda_{j'} - \lambda_j| \lesssim \sqrt{8e}/r, \tag{13}$$

or, in the case of a simple square well, the transitions between the levels are restricted to

$$|j'^2 - j^2| \lesssim \sqrt{8e} h^2/\pi^2 r. \tag{14}$$

Since e is a large number, $1.4 \times 10^5 < e < 9 \times 10^5$, the jumps to a remote level $j' \gg j$ are not only possible but, because of the presence of j' in the preexponential factor in Eq. (11), are very likely.

What happens is illustrated in Fig. 1 which gives the rates of transition from the first level, w_{1j}, and from the 64th level, w_{64j}, Eq. (11), onto all other levels j (the 64th level is chosen because it corresponds to the maximum of w_{1j}) for $r=1.16$,

η=0.116, χ=0.16, and h=5. [The choice of parameters reflects the experimental situation; see below]. The orders of magnitude of w_{1j} and w_{64j} are so vastly different that to have them in the same figure we plotted $10^4 \times w_{1j}$ and w_{64j}. What these data show is that the probability of jump from the first level towards the maximum, $w_{1,64}$, is approximately 10^4 times higher than, for example, for a jump between the first and second levels, $w_{1,2}$. Even more important is that the probability of jump from the 64th level onto, for example, the 82nd, $w_{64,82}$ is also 10^4 higher than for the return from the 64th level to the first level, $w_{64,1}=w_{1,64}$.

All this means that the upward bias in diffusion between the levels is very strong indeed. If a particle starts from the first level, after the first scattering act it will, with overwhelming probability, end up in the state j_1 which is not far away from the maximum of the curve w_{1j} and is much higher than the state j. After the second jump, the particle will be in the state j_2 which is close to the maximum of the curve $w_{j_1 j}$ and is much higher than the state j_1, after the third jump—in the state j_3 near the maximum of $w_{j_2 j}$, and so on. Since the maximum of the curve $w_{j_{n+1},j}(j)$ is always well to the right from the maximum of $w_{j_n,j}(j)$, each step with an overwhelming probability will correspond to an increase in j until the time when the maxima of the curves $w_{j_{n+1},j}$ and w_{j_n},j will be close to each other. As a result, when we are interested in the rates of depletion of the lower levels j_l, for which the maxima of the curves $w_{j_l j}$are well to the right of the values j_l themselves, we can ignore the return processes. The structure of the exponential factors in Eq. (11) means that the maxima on the curves $w_{j'j}(j)$ rapidly shift to the right with decrease in r. For example, when r=0.04, the maximum of the curve w_{1j} shifts from j=64, as at r=1.16, to j=340.

A more accurate equation than Eq. (11) for the interstate transition rates is

$$\frac{1}{\tau_{jj'}} = \frac{1}{\tau_0} w_{jj} = \frac{1}{v_j \hbar^2} \zeta(p-p') U_c^2 \psi_j^2(H) \psi_{j'}^2(H),$$

$$w_{jj'} = 4 \times 10^{-10} u_c^2 b_j b_{j'} \frac{\eta^2 r}{\beta_j} \exp[-(\beta_j - \beta_{j'})^2 r^2/2], \quad (15)$$

where the coefficients b_j are given by the squares of the wave functions on the walls,

$$b_j \equiv 10^5 l_0 \psi_j^2(H)/2. \quad (16)$$

Since the transition rates between the lowest states are much slower than the transitions into the higher states and the values of β_j for the lowest states are almost identical, $\beta_j \approx \sqrt{e}$, the depletion rates for the lowest states, $1/\tau_j$, differ from each other only by the factors b_j and

$$\frac{1}{\tau_j} = \frac{b_j}{b_1} \frac{1}{\tau_1},$$

$$\frac{1}{\tau_1} = \frac{1}{\tau_0} \left(w_1^{(0)} + \sum_{i>1} w_{1i} \right), \quad (17)$$

where

$$w_1^{(0)} = 2 \times 10^{-5} \gamma^2 u_c^2 b_1(h) F_0(\chi, r), \quad \chi = u_c/e, \quad \gamma = \eta/r, \quad (18)$$

$$\sum_{i>1} w_{1i} = 2 \times 10^{-5} \gamma^2 u_c^2 b_1(h) F_1(r,h), \quad (19)$$

$$F_0(\chi, r) = \frac{2r^3\sqrt{\chi}}{\pi} \int_0^{1/\chi - 1} \frac{dz}{\sqrt{z+1}} \times \frac{\exp[-(\sqrt{1/\chi} - \sqrt{1/\chi - 1 - z})^2 u_c r^2/2]}{3 + 1/z}, \quad (20)$$

$$F_1(r,h) = 2 \times 10^{-5} \frac{r^3\sqrt{\chi}}{\sqrt{u_c}} \sum_{i>1} b_i(h) \times \exp[-(\sqrt{1/\chi} - \sqrt{1/\chi - \lambda_i/u_c})^2 u_c r^2/2]. \quad (21)$$

Then Eq. (17) can be rewritten as

$$\frac{\tau_0}{\tau_1} = 2 \times 10^{-5} b_1 u_c^2 \gamma^2 [F_0(\chi, r) + F_1(r,h)], \quad (22)$$

where the first term describes the direct transitions over the absorption threshold and the second the strongly biased upward diffusion.

In the simplest situation, when r is not very small and the jumps from the lowest levels towards the top of the well are restricted, one can use for the higher levels a deep square well approximation,

$$\lambda_j = \pi^2 j^2/h^2,$$

$$\psi_j^2(0) = \psi_j^2(H) = \frac{2}{l_0 h} \frac{\lambda_j}{u_c}, \quad b_j \equiv 10^5 \frac{\lambda_j}{h u_c}, \quad (23)$$

and $F_1(r,h)$ becomes

$$F_1(r,h) = 2 \frac{\pi^2 r^3 \sqrt{\chi}}{h^3 u_c^{3/2}} \sum_{j>1} j^2 \exp[-(\sqrt{1/\chi} - \sqrt{1/\chi - \pi^2 j^2/u_c h^2})^2 u_c r^2/2]. \quad (24)$$

Then the neutron count on the exit counter is equal to

$$\begin{aligned} N_e &= \sum N_j(0) \exp(-L/v_j \tau_j) \\ &= \sum N_j(0) \exp(-L b_j/b_1 \sqrt{e} v_0 \tau_1) \\ &= \sum N_j(0) \exp(-23 \kappa \tau_0 b_j/b_1 \tau_1) \\ &= \sum N_j(0) \exp(-46 \times 10^{-5} u_c^2 z F_1 b_j). \end{aligned} \quad (25)$$

If all initial level occupancies are the same, $N_j(0)=N_0$, then

$$N_e = N_0 f(r,h),$$

$$f(r,h) = \sum \exp(-46 \times 10^{-5} u_c^2 z F_1 b_j). \quad (26)$$

If, as it is indicated by experiments [1], the initial population of the first level is about one-half of the occupancy of the higher ones, the function f should be replaced by

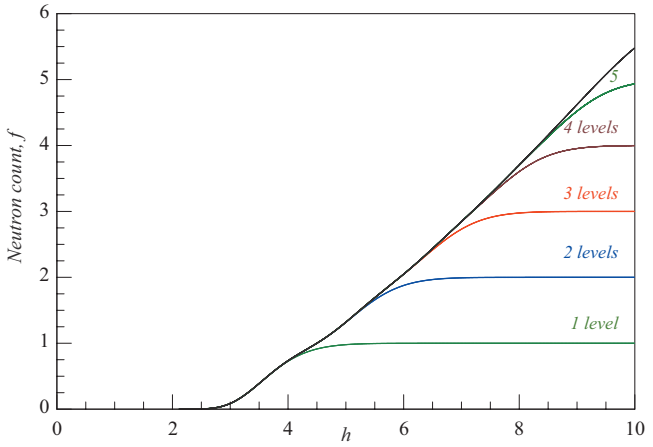

FIG. 2. (Color online) Neutron depletion $f(h)$, Eq. (26), at $r=0.05$, $\chi=0.16$, and $\sigma=1$. The curves labeled *1 level, 2 levels, 3 levels*, etc., give the value of f when the sum in Eq. (26) is restricted to 1, 2, 3, 4, and 5 levels, respectively.

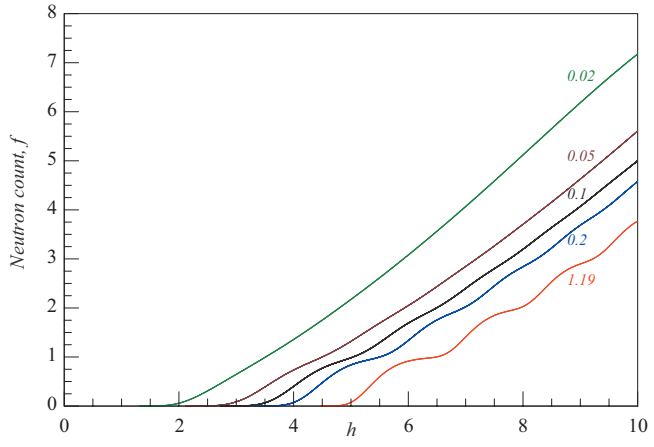

FIG. 3. (Color online) Neutron depletion $f(h)$, Eq. (26), at $\chi=0.16$ and $\sigma=1$ for inhomogeneities of several sizes, $r=1.19,0.2,0.1,0.05,0.02$ for $\eta=r$. The curves are labelled by the values of r. The steps on the curves become more pronounced with an increase in size of inhomogeneities.

$$f_2(x) = \frac{1}{2}\exp(-46\times 10^{-5}u_c^2 z F_1) + \sum_{j>1}\exp(-46\times 10^{-5}u_c^2 z F_1 b_j).$$

IV. BIASED DIFFUSION: RESULTS

The depletion of individual levels as a function of interwall spacing h occurs relatively fast, in a stepwise manner. However, these steps overlap between each other and the overall depletion is a smooth function of h. This is illustrated in Fig. 2. Here we plotted function $f(h)$, Eq. (26), which gives the normalized neutron count at $r=0.05$, $\chi=0.16$, and $\sigma=1$. The curves labeled *1 level*, *2 levels*, *3 levels*, etc., give the value of f when the sum in Eq. (26) is restricted to 1, 2, 3, etc., levels only. This figure clearly demonstrates that though individual levels depopulate rather abruptly, in a stepwise manner, the overall depletion $f(h)$ remains smooth.

A surprising observation is that the overall neutron count for coarser roughness—i.e., for larger η and r—acquires a stepwise character (see Fig. 3), which is an obvious sign of the quantum size effect in neutron count. In this figure we plotted function $f(h)$, Eq. (26), at $\chi=0.16$ and $\sigma=1$ for inhomogeneities of several sizes $\eta=r$. The stepwise nature of the curve at larger values of η and r is unmistakable. This presents a stark contrast to the results of Ref. [8] according to which the observation of the steps for direct absorption processes, which dominate at very small r, can be observed only for $\sigma \gtrsim 400$. This contrast is explained partially by the fact that the larger values of r allow one to use roughness with the higher amplitude η while still remaining in the low-roughness domain $\eta \ll r,1$. However, the overall effect is related mostly to the contribution of the intermediate states to the level depletion.

In order to illustrate the fact that the sharpness of the quantum size effect in neutron count is related to the increase in roughness amplitude η rather than to the lateral size of inhomogeneities r, in Fig. 4 we present the data for the neutron depletion at various, rather large values of r, $r=1,2,5,10,20$ but, in contrast to Fig. 3 in which the amplitude of inhomogeneities was the same as their lateral size, at constant value of the amplitude, $\eta=0.5$. As one can see, the sharpness of the steps remains more or less the same irrespective of the value of the correlation radius r.

Another major difference from the results of Ref. [8] is the dependence of the neutron depletion on the ratio χ of the absorption threshold energy U_c to the overall energy E. The direct absorption processes are extremely sensitive to this ratio which determines how large the scattering-driven rotation of velocity should be in order for the particle to get absorbed directly. In the case of biased diffusion, which is described above, this ratio is largely irrelevant: here the main part of the absorption process is spent on the first jump—i.e.,

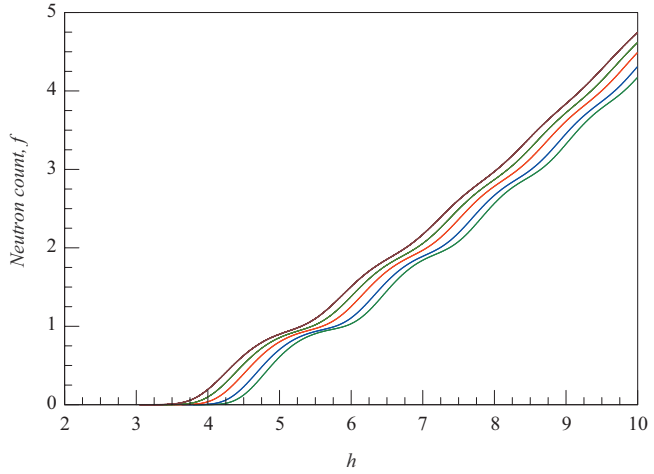

FIG. 4. (Color online) Neutron depletion $f(h)$, Eq. (26), at $\chi=0.16$ and for inhomogeneities of several sizes r, $r=1,2,5,10,20$ and the same amplitude of the inhomogeneities, $\eta=0.5$. The higher curves correspond to larger values of r. The sharpness of the steps remains the same irrespective of r.

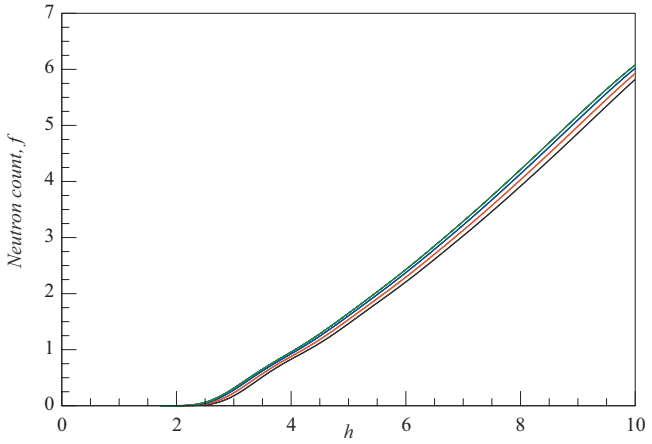

FIG. 5. (Color online) Neutron depletion $f(h)$, Eq. (26), at $r=0.04$ and $\sigma=1$ for several values of the threshold ratio χ, $\chi=0.16, 0.3, 0.5, 0.7$. Higher curves correspond to larger values of χ.

on the transition from the initial state to some higher state, rather than on the transition from this higher state to the continuum. In this case, the weak dependence of the depletion rate on χ appears only because χ affects the time of flight t and, to a lesser degree, a number of transitions necessary for absorption. This weak dependence of the neutron depletion on the threshold ratio χ is consistent with the experimental data and is illustrated in Fig. 5 for inhomogeneities with $r=0.04$. In this figure, higher curves correspond to larger values of χ though the curves are almost indistinguishable. This somewhat counterintuitive dependence on $\chi=U_c/E$ is explained by the dependence of the correlation exponent in Eq. (21) on χ.

The dependence of the neutron count on the parameter σ is more noticeable, partially because σ, which is proportional to the square of the ratio of the height and the lateral size of inhomogeneities, can change in a much wider range than χ. The dependence of the neutron count on σ is illustrated in Fig. 6 for $r=0.04$. This relatively strong dependence of the neutron count on σ is very unfortunate since the experimental value of σ is often unknown precisely. However, if one does not make special efforts to prepare inhomogeneities with lateral and transverse sizes of vastly different scales, a natural assumption is that σ for a random rough surface is of the order of 1.

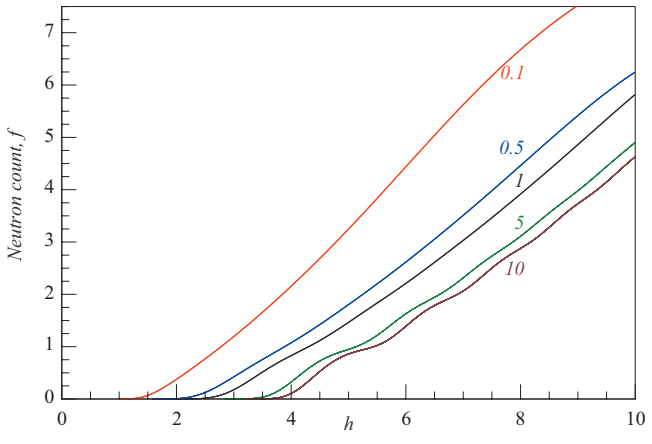

FIG. 6. (Color online) Neutron depletion $f(h)$, Eq. (26), at $r=0.04$ and $\chi=0.16$ for several values of σ, $\sigma=0.1, 0.5, 1, 5, 10$. The curves are labeled by the values of σ.

V. EXACT DESCRIPTION OF NEUTRON DEPLETION AND THE ACCURACY OF THE BIASED DIFFUSION MODEL

When the correlation radius (lateral size) of surface inhomogeneities r increases, the correlation-driven exponential factor

$$\exp[-(\beta_j-\beta_{j'})^2 r^2/2] \tag{27}$$

in the transitional probabilities $w_{jj'}$, Eq. (15), limits the transitions to the nearby states and the peaks in $w_{jj'}(j')$, such as the ones in Fig. 1, shift more and more to the left. The closer is the maximum of the curve $w_{jj'}(j')$ to the starting point j, the smaller is the upward bias in the interstate diffusion. This means that the upward bias in the scattering-driven interstate diffusion decreases with growing coarseness of the mirror corrugation r. As a result, the biased diffusion model from the previous sections may lose its accuracy at larger r. Therefore, at large values of the correlation radius of inhomogeneities r we have to solve the transport equation exactly. This will also provide us with a good estimate of the accuracy of the bias diffusion model.

An estimate of the correlation-driven limitation on the length of a likely jump $j\to j'$ is given by Eq. (15),

$$j'^2 \sim j^2 + \sqrt{8e}h^2/\pi^2 r. \tag{28}$$

Since the kinetic energy of the motion along the slit, e, is much higher than the typical gravitational energies inside the slit, jumps to high energy levels $j' \gg j$ are possible for $r \lesssim \sqrt{8e}h^2/\pi^2 \sim 250h^2$ at $\chi=0.16$. When r is smaller than this very large number, the accuracy of the biased diffusion model should be excellent.

In order to check the accuracy of the biased diffusion model, we solved the full transport equation numerically at several large values of r, such as those in Fig. 4, while keeping the amplitude of inhomogeneities constant an relatively small, $\eta=0.5$, and compared the data with the biased diffusion results. Not surprisingly, there was no noticeable difference between the biased diffusion and exact computations. There is no reason even to plot these data.

At higher values of r the computation times increase dramatically and, what is worse, the numerical solution of the full transport equation starts to lose stability. The culprit is the structure of the matrix of transition probabilities which contains the exponents (27) with prefactors of the type $j^2 j'^2$. With increasing r, this matrix becomes more and more disbalanced with respect to the *antidiagonal* with the elements below the *antidiagonal* being larger by many orders of magnitude than the ones above it. Simple brute force enhancements, such as doubling the precision or rearranging the matrix, do not let us extend the computations reliably beyond $r=15$. Fortunately, it looks unlikely that the experiments will be performed using mirrors with very large values of r.

Though this computational issue in solving the exact transport equation can be overcome, we prefer, instead, to calculate the iterative corrections to the biased diffusion results from the previous section.

We look for a solution of the full transport equation in the form

$$N_j(t) = \tilde{N}_j(t) a_j(t), \tag{29}$$

where $\tilde{N}_j(t) = N_0 \exp(-t/\tau_j)$ are the time dependences of the level occupancies from the biased diffusion calculations of the previous section. Since the biased diffusion approximation takes into account only transitions away from the levels and neglects the return processes, the exact equations for the correction coefficients $a_j(t)$ have the form

$$\tilde{N}_j(t)\frac{da_j}{dt} = \frac{1}{\tau_0}\sum_{j' \neq j} \frac{\beta_j w_{jj'}}{\beta_{j'}} \tilde{N}_{j'}(t) a_{j'}(t), \quad a_j(t=0) = 1. \tag{30}$$

The first iteration to the solution is obtained by replacing $a_{j'}(t)$ on the right-hand side (RHS) of this equation by 1,

$$a_j(t) = 1 + \frac{\tau_j}{\tau_0} \sum \frac{\beta_j w_{jj'}}{\beta_{j'}} \frac{\tau_{j'}}{\tau_j - \tau_{j'}} \left[1 - \exp\left(\frac{t}{\tau_j} - \frac{t}{\tau_{j'}} \right) \right], \tag{31}$$

and the correction coefficients at the time when the neutrons reach the exit counter are

$$a_j(L/v) = 1 + \delta a_j, \quad \delta a_j = \frac{\tau_j}{\tau_0} \sum \frac{\beta_j w_{jj'}}{\beta_{j'}} \frac{\tau_{j'}}{\tau_j - \tau_{j'}} \left[1 - \frac{\tilde{N}_{j'}}{\tilde{N}_j} \right], \tag{32}$$

where $\tilde{N}_j$ are the occupancy numbers at the exit counter in the biased diffusion approximation. The next iteration is obtained by replacing $a_{j'}(t)$ on the RHS of Eq. (30) by the value given by Eq. (31), etc. Since $\tilde{N}_j(t)$ are simple exponential functions, this iterative procedure is computationally transparent.

For example, the first iteration for the correction coefficient for the population of the lowest state is

$$\delta a_1 = \frac{\tau_1}{\tau_0} \sum_{j>1} \frac{\beta_1 w_{1j}}{\beta_j} \frac{\tau_j}{\tau_1 - \tau_j} \left[1 - \frac{\tilde{N}_j}{\tilde{N}_1} \right] \tag{33}$$

or, according to Eq. (17),

$$\delta a_1 = \left(w_1^{(0)} + \sum_{i>1} w_{1i} \right)^{-1} \sum_{j>1} \frac{\beta_1 w_{1j}}{\beta_j} \frac{\tau_j/\tau_1}{1 - \tau_j/\tau_1} \times \left[1 - \exp\left(\frac{23\tau_0(\tau_j/\tau_1 - 1)}{\tau_j} \right) \right], \tag{34}$$

where we used the same numerical value for $L/v\tau_0 \approx 23$ as in the computations in the previous section. Since the main contribution to the sum comes from the area of the peak in Fig. 1 and not from the lowest levels, one cannot use here the approximation b_1/b_j for the ratios τ_j/τ_1 inside the sum. On the other hand, for all higher levels the occupancies $\tilde{N}_j/\tilde{N}_1 \ll 1$ and the corresponding exponents in Eq. (34) can be disregarded. It is, therefore, obvious that this correction never exceeds

$$\delta a_1 < \frac{\tau_1}{\tau_0} \sum_{j>1} \frac{\beta_1 w_{1j}}{\beta_j} \frac{\tau_j}{\tau_1 - \tau_j} \tag{35}$$

and should be quite close to this value.

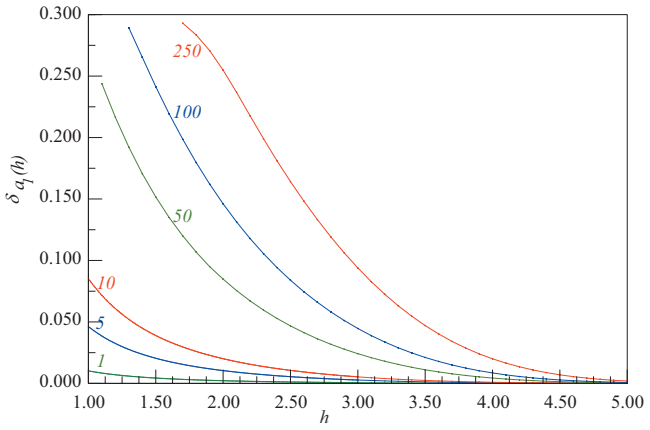

FIG. 7. (Color online) Correction coefficient $\delta a_1(h)$, Eq. (34), for $r=1,5,10,50,100,250$ and $\eta=0.5$. The curves are marked in accordance with the values of r.

The correction coefficient $\delta a_1(h)$, Eq. (34), is plotted in Fig. 7 for six values of r, $r=1,5,10,50,100,250$. For $r<1$ the correction coefficients cannot even been seen on this scale. The correction coefficients for the occupancies of higher levels, $\delta a_{j>1}(h)$, are somewhat higher. However, one should keep in mind that these levels are depleted much faster than the first level and the corresponding corrections $\delta a_j \tilde{N}_j$ to the overall neutron count are quite small even when δa_j are noticeable.

Figure 7 confirms the conclusions of the beginning of this section that the corrections to the biased diffusion results are negligible for mirrors with inhomogeneities of small and moderate lateral sizes r. Note that the parameters $\eta=0.5$ and very large $r=250$ describe mirrors with roughness of amplitude 2.9 μm and unrealistic lateral size 1.5 mm. In principle, systems with very large values of r may also exhibit an anomalous quantum size effect of the type [9] which is associated with the spontaneous opening of interstate transition channels. This possibility and its implications will be discussed elsewhere.

Since the computation times for exact solution of the transport equation are much longer than those for the biased diffusion model, the only conclusion is that a proper computational procedure for analysis of experiment is a rapid scan of a wide parameter range using the biased diffusion model supplemented by the exact solution of the transport equation in the most important points. When the correlation radius of inhomogeneities is large, $r>15$, a better alternative to the exact solution is the iterative computation of the correction coefficients in accordance with the above scheme.

VI. COMPARISON WITH EXPERIMENT

Before starting a detailed comparison with experimental data, one should analyze the limitations of the theoretical calculations and the effect of uncertainty of the input parameters, which come from experiment, on the results.

A. Roughness-driven broadening and shift of the gravitational states

Up to now we assumed that the gravitational states are well-defined energy levels. At first glance, surface roughness should lead to a broadening and shifting of these levels. Strictly speaking, this is not entirely true and the situation is more complicated. Though we use the term "gravitational level" to describe the quantization of neutrons by the gravitational field, one should keep in mind that in reality we are dealing with 3D particles in a 1D quantizing field. This means that the solution of the Schrödinger equation is not just a set of discrete energy levels ϵ_j, but a set of 2D "gravitational" energy bands $\epsilon_j+p^2/2m$, and we are dealing, effectively, with a continuous spectrum. In the case of a continuous spectrum, any perturbation, including the roughness-driven one, leads not to distinct energy shifts and line broadening, but to a mixing of the states of the type that we calculated in the previous sections.

The notion of an individual energy band makes sense only if the roughness-driven mixing of the bands is not too large. This means that the effective broadening

$$\delta\epsilon_j \sim \hbar/\tau_j$$

should be much smaller than the separation between the bands,

$$\delta\epsilon_j \ll \epsilon_{j+1} - \epsilon_j.$$

Since the line broadening for the square well levels is proportional to j^2 and the distance between the nearby levels increases only proportionally to j, the first bands to overlap are the upper ones with

$$\delta\epsilon_j \sim \frac{\hbar^2}{m}\frac{\pi^2 j}{H^2}$$

or, what is the same,

$$\frac{\hbar}{\tau_j e_0} \sim 2j\frac{\pi^2}{h^2}, \tag{36}$$

with τ_j given by Eqs. (17)–(22),

$$\frac{\tau_0}{\tau_j} = 2\times 10^{-5} b_j u_c^2 \gamma^2 [F_0(\chi,r) + F_1(r,h)]. \tag{37}$$

Then the critical value of j, above which the bands overlap with each other, is

$$1/j_c \sim 9.5\times 10^{-7} u_c \gamma^2 [F_0(\chi,r) + F_1(r,h)]/h. \tag{38}$$

Numerical evaluation shows that the value of j_c is almost always linear in h,

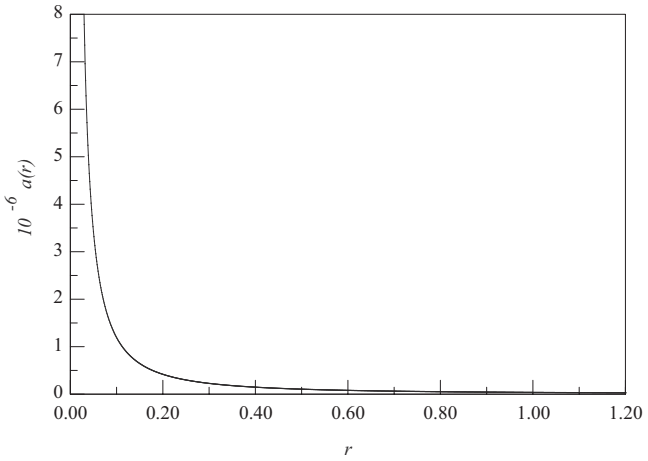

FIG. 8. Plot of function $10^{-6}a(r)$, Eq. (39).

$$j_c \approx a(r)h/\gamma^2, \tag{39}$$

with very large a, $a(r=0.04)\approx 4.9\times 10^6$, $a(r=0.2)\approx 4.2\times 10^5$, and $a(r=0.04)\approx 2.9\times 10^4$. A plot of the function $10^{-6}a(r)$ is given in Fig. 8. Since the overall number of levels is of the order of 10^4h^2, the broadening of the *highest* levels is important only when the ratio of the amplitude of roughness to its lateral size, $\gamma=\ell/R$, is large (and even then only at relatively large values of the spacing h and coarse inhomogeneities with $r\gtrsim 1$). The broadening of the lower levels is negligible except for the walls with very strong roughness. Therefore, the influence of the level broadening on the neutron depletion can be largely ignored.

There is still a question whether the values of ϵ_j, which determine the quantized energy bands $\epsilon_j+p^2/2m$, are well defined. The exact values of ϵ_j are of paramount importance if one is serious about using gravitationally quantized neutrons for measuring the fundamental forces in the μm range [3–5]. One of the main sources of uncertainty in ϵ_j is driven by a purely practical consideration. With increasing roughness, it is getting more difficult to determine experimentally the exact *average* position of the mirror and, therefore, the exact spacing h. In many typical experiments the uncertainty in h is somewhere in between 0.1 and 0.2. Since the values of the energy levels depend strongly on the spacing between the walls, this uncertainty in h leads to an uncertainty in the energy values. For example, Fig. 9 presents the uncertainty bands for the lowest nine (dimensionless) energy levels $\lambda_j=\epsilon_j/e_0$ that correspond to uncertainty ± 0.1 in the value of the wall spacing h.

As one can see from the figure, the uncertainty in the level positions is quite high and is comparable to the distance between the levels, especially at low spacings $h<5$ that correspond to the main experimental range. If the uncertainty in h reaches 0.2, the uncertainty bands for different levels start overlapping with each other. This does not imply that the individual levels intersect with each other: all the levels shift in a systematic way in the same direction. What it means is that the identification of the energy states can become unreliable while their energies become highly uncertain. The experimental uncertainty in h degrades the quality of the data

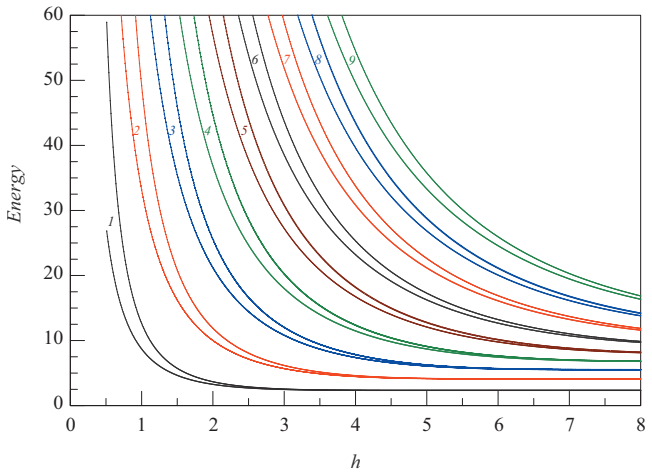

FIG. 9. (Color online) Uncertainty bands for the lowest nine gravitational states between the walls $\lambda_j=\epsilon_j/e_0$ that correspond to uncertainty ±0.1 in the value of the wall spacing h.

and requires using an offset when interpreting the experimental data as is done below.

B. Initial distributions

One of the most important issues is the initial distribution of neutrons over the gravitational states, $N_j(t=0,h)$. In experiment, the measured quantity is the dependence of the neutron flux after it passes the rough slit on the slit width h. This flux is equal to

$$N(t,h)=\sum N_j(t=L/V,h)\sim\sum N_j(0,h)\exp(-L/V\tau_j). \tag{40}$$

Unfortunately, neither the absolute values of the individual initial occupancies $N_j(0,h)$ nor even their relative values are known experimentally with good accuracy. Although such measurements are, in principle, possible, they are too complicated and time consuming and have not been done yet. A reliable calculation, which would be based on the known data on neutron distributions in front of the collimators and would include all diffraction effects for a realistic cell, is also, in principle, possible, but seems even less likely.

A natural assumption is that, since the distribution of the particles over the vertical velocities in the feeder beam before it enters the slit is nearly flat, the initial occupancies of the *lowest* states are the same, $N_j(0,h)=n$ and

$$N=n\sum\exp(-L/V\tau_j). \tag{41}$$

Even though the value of n is not known exactly, we can use it as a fitting parameter by fitting one of the points of the experimental curve $N(h)$ to the theoretical curve. The best candidate here is the point at the highest value of h since the neutron count and, therefore, the accuracy of measurements increase with increasing clearance between the walls h. This procedure was used when comparing our results to experimental data.

Such a fitting procedure relies on two assumptions. The first one is, of course, that the initial occupancies of all states are the same, $N_j(0)=n(h)$. The second implicit assumption is that the relative distribution of the neutrons over the states does not change with change in h, $n(h)=n$. A brief theoretical analysis [4] seems to confirm the first assumption. However, even if the first assumption $N_j(0)=n$ holds for all values of h, this does not automatically mean that the value of n does not depend on h.

In addition, there are some experimental indications that the occupancy of the lowest gravitational state is lower than that for the higher states [1], but the spatial resolution of the corresponding measurements is too low to make any definite conclusions.

We analyzed this issue assuming that the distribution of neutrons in the feeder beam, before it enters the slit, over the "vertical" kinetic energies is flat or Gaussian. Since we are interested only in the lowest states with energies in the peV range, these two situations are identical for all practical purposes.

One of the main sources of uncertainty for the initial distribution of particles over the lowest gravitational states is the distribution of particles over the vertical velocities in the feeder beam after the beam passes the collimators. (The distribution in front of collimators was measured and turned out to be uniform. Using these data, the distribution behind the collimators can, in principle, be calculated; however, an accurate calculation, including all diffraction effects, is too complicated). There are two natural assumptions: either the distribution of particles in the feeder beam over the vertical momenta q is a constant, $n_q(q\to 0)=\text{const}$, or the distribution over the corresponding kinetic energies is constant, $n_\epsilon(\epsilon\to 0)=\text{const}$. The former case seems to be closer to experimental data though the latter one corresponds to the equilibrium distribution. Since $d\epsilon=qdq/m$, these two distributions are drastically different at low momenta, $n_q=n_\epsilon q/m$.

The initial occupancy of the quantum level j between the plates can be estimated as

$$N_j=\sum_m n_m\left|\int\Psi_m^*(x)\psi_j(x-y)dx\right|^2, \tag{42}$$

where $\Psi_m(x)$ and $\psi_j(x-y)$ are the wave functions in the feeder beam and inside the slit with the parameter y characterizing the displacement of the bottom of the slit with respect to the bottom of the feeder beam, and n_m is the distribution over states m in the feeder beam. We evaluated the occupancy as a function of the quantum number j without and with the gravitational field. In the former case, we looked at a wide rectangular feeder beam of width L entering a narrow slit of width $h\ll L$; in the latter case, the width of the feeder beam was determined by the gravitational energy cutoff. The findings in both cases are similar. In general, the initial occupancies of all states are the same and do not depend on the well width h except for the smallest values of h at which the occupancies experience a sharp drop. The origin of this drop is rather obvious. The energy states inside the well are rapidly going up with decreasing h (as $1/h^2$ in the absence of the gravitational field) and the distance between the nodes of the wave function drops proportionally to h. Therefore, at smaller h one needs higher and higher terms in

the summation (42) over the states of the feeder beam in order to get the "full" occupancy of the state j. Since there is an inevitable high-energy cutoff in the feeder beam, there is a certain critical value of h below which there is simply not enough terms in the sum (42) in order to maintain the full occupancy of the well states j; the higher is this cutoff, the lower is the critical value of h. For all realistic values of the energy cutoff in the feeder beam, the drop in initial occupancy starts at $h \lesssim 1$. It is also obvious that this critical width h should increase with increasing level number j.

In the presence of the gravitational field, one can choose the semiclassical gravitational functions for the states Ψ_m in the feeder beam with energies μ_m,

$$\Psi_m(x) = \frac{\mathrm{Ai}(x-\mu_m)}{\mathrm{Ai}'(-\mu_m)}, \quad \mu_m = \left[\frac{3\pi}{4}\left(2m-\frac{1}{2}\right)\right]^{2/3}, \quad (43)$$

and for $\psi_j(x-y)$ the wave functions from Ref. [8]. Assuming that the neutrons in the feeder beam are uniformly distributed over the *energies* μ in the vertical direction $n(\mu)$ in some interval Δ, $n(\mu)=N/\Delta$, the distribution over the quantum numbers is

$$n_m = \frac{\pi N}{\Delta\sqrt{\mu_m}} \quad (44)$$

and Eq. (42) reduces to

$$N_j = \frac{N\pi}{\mu_b - \mu_a}\frac{\nu_j}{\sqrt{\mu_0}},$$

$$\nu_j = \sqrt{\mu_0}\sum_{m_0-a}^{m_0+b}\frac{1}{\sqrt{\mu_m}}\left|\int \Psi_m^*(x)\psi_j(x-y)dx\right|^2, \quad (45)$$

where $\mu_0=\left[\frac{3\pi}{4}\left(2m_0-\frac{1}{2}\right)\right]^{2/3}$ is the gravitational energy at the bottom of the slit. On the other hand, if the distribution over the vertical *velocities* in the feeder beam is uniform, then the occupancies of the gravitational states in the slit are slightly different,

$$N_j = \frac{N\pi/2}{\sqrt{\mu_b}-\sqrt{\mu_a}}\frac{\nu_j}{\mu_0},$$

$$\nu_j = \mu_0\sum_{m_0-a}^{m_0+b}\frac{1}{\mu_m}\left|\int \Psi_m^*(x)\psi_j(x-y)dx\right|^2. \quad (46)$$

It turns out that both occupancies ν_j, Eqs. (45) and (46), are similar to each other and are equal to 1 except for the smallest values of $h \lesssim 1$. For example, Fig. 10 presents the initial occupancies (45) $\nu_j(h)$ for the lowest nine gravitational levels when $m_0=1007$, $a=300$, and $b=5000$. The critical values of h, at which the occupancies start going down, are not sensitive to the parameter a, but are sensitive to m_0 and b: with an increase in b or a decrease in m_0 the critical values of h decrease.

The computational results for ν_j in the case of a uniform distribution over velocities, Eq. (46), are practically the same. If the distribution of particles in the feeder beam is not flat but Gaussian, the drop in the occupancies ν_j starts at higher values of widths h. The steeper is the Gaussian distribution in the feeder beam, the more spread out are the curves $\nu_j(h)$.

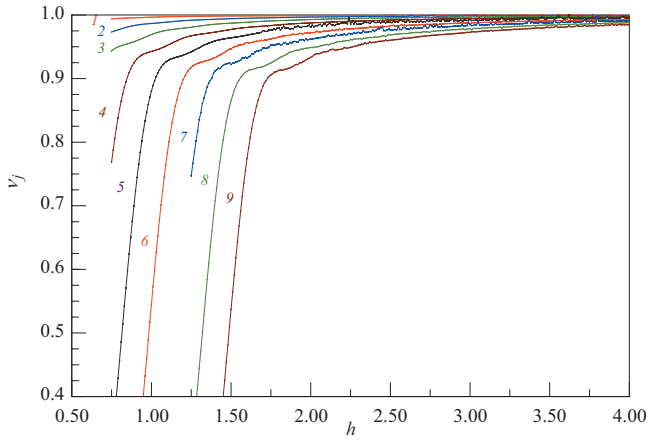

FIG. 10. (Color online) Initial occupancies of the gravitational states between the plates $\nu_j(h)$, Eq. (45), for the lowest nine levels when $m_0=1007$, $a=300$, and $b=5000$. The critical values of h, at which the occupancies start to drop, decrease with decrease in m_0 and increase with the energy cutoff in the feeder beam b.

Unfortunately, most of the feeder beam parameters in Eqs. (45) and (46) are unknown though it is reasonably safe to assume that in most of the experimental domain the gravitational levels experience considerable roughness-driven depletion at higher values of h than those for which the initial occupancies $\nu_j(h)$ start to drop. Therefore, our only conclusion from the above analysis is that the initial occupancies of all levels are the same and do not depend on the spacing between the plates h, $\nu_j=1$ and $N_j(0)=n=\mathrm{const}$. The numerical value of n is, nevertheless, unknown. Also, we are not able to confirm or explain the observation [1] that the initial occupancy of the ground state seems to be lower than that for the higher states.

The experimental data yield the absolute value for the neutron count:

$$N = \sum N_j(t).$$

Our results express the final populations of the gravitational states, $N_j(t)$, via their initial populations $N_j(0)=n$. Since the initial population of each state n is unknown, the only way to compare the experimental and theoretical results is to choose the value of n by fitting one of the experimental points to the curve $f(h)$, Eq. (26), or a similar curve from Sec. IV. The best choice for such a fitting point is the point with the highest neutron count (the largest h) where the experiment has the highest accuracy.

C. Comparison with experiment

Figure 11 compares the best published experimental data (the third Ref. [1]) with our calculations. According to experimental observations, the correlation radius (lateral size) of the surface inhomogeneities was $r=1.19$ ($R\approx 7$ μm) and the amplitude (height) of inhomogeneities was 10 times smaller, $\eta=0.119$ ($\ell\approx 0.7$ μm) (i.e., $\sigma=0.01$). The fit was

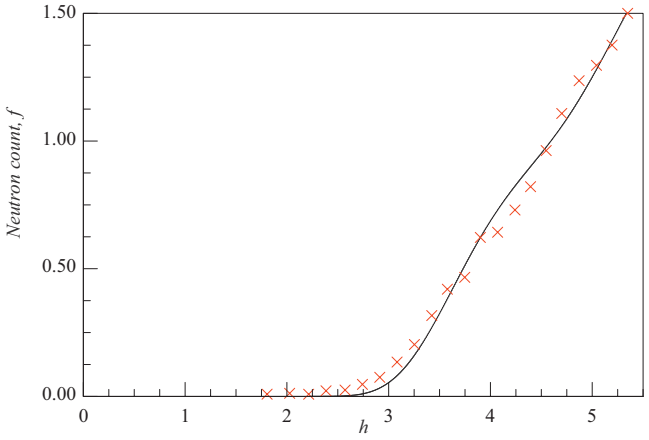

FIG. 11. (Color online) Comparison of neutron depletion calculations $f(h)$, Eq. (26) (solid line) with experimental data (crosses) of the third reference in Ref. [1]. Calculations use the experimental estimates $r \approx 1.19$ ($R \approx 7$ μm) and $\eta \approx 0.119$ ($\ell \approx 0.7$ μm).

done using the information on initial occupancies from the previous subsection, $\nu_j = 1$. The fit also includes the offset of 1.6 μm ($\delta h \approx 0.27$) in the width of the slit [1].

The agreement between theoretical and experimental results is amazingly good especially if one takes into account a not very high accuracy (10%–20%) of the experimental estimates of roughness. This quality of the fit is especially striking because of a high sensitivity of the theoretical curves to the amplitude and correlation radius of the surface inhomogeneities η and r. If the ratio η/r were equal to 1, and not 0.1 as in experiment, the same quality of fit could have been achieved only at $r = 0.04$.

VII. CONCLUSIONS

We developed a comprehensive theory of transport of gravitationally quantized neutrons in a rough absorbing waveguide. The results are in a very good agreement with experimental data, much better than in our previous attempt [8] to describe the Grenoble experiment and with much fewer free parameters than Ref. [10]. Our only remaining free parameter—the state occupancy for entering neutrons—can also be eliminated in future experiments.

In contrast to our earlier calculations [8], which took into account only direct scattering-driven absorption processes, the calculation includes all possible indirect depletion processes occurring via intermediate states. The computations were done by both solving the full transport equation encompassing all transitions and using a much more transparent and time-efficient-biased diffusion model. The agreement between both approaches, which is generally very good in the whole parameter range, becomes perfect for rough mirrors with small and moderate radii of surface roughness. This means that any future analysis of the quantum size effect for gravitationally quantized neutrons can be done by a rapid scanning of the interesting parameter range using the semi-analytical biased diffusion model with a consecutive exact solution of the full transport equation in the most important points.

Our biased diffusion model assumes that the scattering-driven diffusion of neutrons through the set of quantized energy levels has a strong upward bias with neutrons rarely, if ever, going to the lower-energy states. This allows us to avoid diagonalizing the full matrix of transition probabilities involving hundreds of discrete quantized states and to get a transparent analytical expression for the neutron depletion rate.

We also studied in detail several factors that affect analysis of experimental data and are important for potential applications of quantum size effects in neutrons for measuring fundamental forces in the sub-μm range [5]. The most important factors are the experimental uncertainty in the waveguide width, which increases with an increase in the amplitude of roughness, and the lack of reliable experimental information on the initial population of the quantum states. The former factor results in an uncertainty in the energy calibration while the latter one necessitates the use of the only fitting parameter in comparing theoretical and experimental results. Although the initial populations can, in principle, be calculated from the measured neutron distribution in front of the collimators, such a calculation is extremely complicated and is hardly realistic. The measurement of the neutron distribution in front of the mirrors (slit), but after the beam passes through all the collimators seems as a better option than the calculation involving all possible diffraction effects. Another desirable measurement would be a more accurate study of the mirror inhomogeneities using some of the standard experimental techniques in dealing with random rough surfaces [11].

We demonstrated that there exists a clearly identifiable parameter range in which one can observe the quantum size effect—namely, the distinct quantum steps in the exit neutron count—even for waveguides with weak roughness, $\ell \lesssim R, l_0$. The sharpness of the quantum size effect increases with an increase in the amplitude of the surface inhomogeneities ℓ and is not very sensitive to their lateral size R. The limitations on the experimental observation of the very sharp steps are caused mostly by the loss of energy resolution with increasing amplitude of inhomogeneities.

Our results identify the most advantageous parameter range for the observation of the quantum size effect for the gravitationally quantized neutrons in a rough waveguide, without degrading the quality of the energy calibration. Just a threefold increase of the amplitude in roughness for an existing waveguide with $r = 1.19$, which can easily be done experimentally, seems to be sufficient for an unmistakable resolution of the quantum steps.

ACKNOWLEDGMENT

One of the authors (A.M.) is grateful to the ILL group for the hospitality during his stay in Grenoble and for stimulating discussions. One author (V.M.) is grateful to the French Agence Nationale de la Recherche (ANR) for support of GRANIT project at ILL.

[1] V. V. Nesvizhevsky *et al.*, Nature (London) **415**, 297 (2002); V. V. Nesvizhevsky *et al.*, Phys. Rev. D **67**, 102002 (2003); V. V. Nesvizhevsky *et al.*, Eur. Phys. J. C **40**, 479 (2005) (for an additional bibliography see also http://lpscwww.in2p3.fr/UCN/NiveauxQ-G/publications/index.html).

[2] J. H. Freed, Ann. Phys. (Paris) **10**, 901 (1985).

[3] H. Murayama, G. G. Raffelt, C. Hagmann, K. van Bibber, and L. J. Rosenberg, in *Review of Particle Properties*, K. Hagiwara (Particle Data Group) [Phys. Rev. D **66**, 010001 (2002)].

[4] V. V. Nesvizhevsky and K. V. Protasov, Class. Quantum Grav. **21**, 4557 (2004).

[5] Possible use of gravitational quantization of neutrons for measuring the fundamental forces was the main topic of the workshop http://lpsc.in2p3.fr/congres/granit06/index.php(ILL, Grenoble, 2006).

[6] A. E. Meyerovich and A. Stepaniants, Phys. Rev. B **60**, 9129 (1999).

[7] I. M. Lifshitz, S. M. Gredeskul, and L. A. Pastur, *Introduction to the Theory of Disordered Systems* (Wiley, New York, 1988).

[8] A. E. Meyerovich and V. V. Nesvizhevsky, Phys. Rev. A **73**, 063616 (2006).

[9] A. E. Meyerovich and I. V. Ponomarev, Phys. Rev. B **65**, 155413 (2002); Y. Cheng and A. E. Meyerovich, *ibid.* **73**, 085404 (2006).

[10] A. Yu. Voronin, H. Abele, S. Baeszler, V. V. Nesvizhevsky, A. K. Petukhov, K. V. Protasov, and A. Westphal, Phys. Rev. D **73**, 044029 (2006).

[11] J. A. Ogilvy, *Theory of Wave Scattering from Random Surfaces* (Adam Hilger, Bristol, 1991).